RSC Advances

PAPER

View Article Online
View Journal | View Issue

Check for updates

Cite this: *RSC Adv.*, 2026, **16**, 28917

Refractometric and conductivity based water cut measurement techniques for stable emulsions

Mabkhot BinDahbag, Dennis Atta and Hassan Hassanzadeh *

The production stream from thermal recovery processes for heavy oil and bitumen, such as steam-assisted gravity drainage, contains highly stable emulsions. The precise measurement of water cut in produced stable emulsions is essential for making informed economic and management decisions, yet it remains a complex challenge. This study introduces novel measurement techniques by applying Boyle's law in combination with RI or EC to measure water cut in stable emulsions. To accurately measure the volume of the aqueous phase in a stable emulsion, a known amount of salt, such as NaCl, is added. The salinity of the extracted brine is then assessed using RI or EC. By correlating the added NaCl weight with the measured salinity, the water volume in the emulsion—and consequently, the water cut—can be precisely determined without separating water from the oleic phase. With accurate measurements of the total volume of the emulsion and the volume of the aqueous phase in the emulsion, the water cut and volume of the oleic phase can be determined precisely. The developed measurement techniques were first validated using known emulsion samples and then applied to measure the water cut in unknown stable emulsion samples from an ES-SAGD experiment. The results showed excellent agreement with those obtained using the centrifuge method.

Received 13th April 2026
Accepted 19th May 2026

DOI: 10.1039/d6ra03130g

rsc.li/rsc-advances

Open Access Article. Published on 27 May 2026. Downloaded on 5/30/2026 4:58:45 PM.
This article is licensed under a Creative Commons Attribution-NonCommercial 3.0 Unported Licence.

1. Introduction

Water cut (WC) measurement is a critical parameter in the petroleum industry, influencing every stage of operations, from oil exploration and development planning to production, transportation, storage, marketing, and refining. Its significance lies in its ability to assess reservoir productivity, guide well completion design, optimize well placement, and enhance production efficiency. Additionally, it plays a key role in planning Enhanced Oil Recovery (EOR) strategies, determining the need for corrosion inhibitors for pipelines and storage tanks, and ensuring that oil quality meets industry standards for marketing and refining.[1,2]

Water-cut measurement methods fall into two main categories: offline and online methods.[3] Offline methods involve collecting representative samples from the oil production stream and analyzing water content in a laboratory using techniques such as the distillation method (Dean–Stark), centrifugation, and Karl-Fischer titration.[4] These methods are valued for their simple design, low sensitivity to emulsification, and cost-effectiveness. Most offline techniques rely on physically separating water from the oil phase for the entire sample, except for the Karl-Fischer titration, which determines water content by measuring the reaction of iodine (I_2) with water in the presence of sulfur dioxide (SO_2) and an alcohol base such as methanol (CH_3OH).[5]

Despite their advantages, offline methods have notable drawbacks. They are time-consuming, require separation of water from oil, and are labor-intensive, making them less suitable for real-time monitoring. Accuracy can also be compromised if the sample does not fully represent the emulsion as a whole. Furthermore, distillation-based techniques are prone to losing volatile components, potentially leading to measurement errors.[3]

In contrast, online water-cut measurement methods provide real-time monitoring by directly analyzing the flowline stream. Various advanced techniques have been developed for this purpose, including capacitance-based meters, tomography-based meters, gamma densitometry, infrared sensors, Coriolis flowmeters, ultrasonic meters, microwave sensors, and the conductance method. Each technique offers unique advantages and limitations, making them suitable for different operational conditions and measurement requirements.[6]

Capacitance-based water-cut meters measure the dielectric properties of water-in-oil (W/O) emulsions in which the oil is the continuous phase. However, the relationship between dielectric properties and water content becomes nonlinear when water levels exceed 10 vol%.[7] These meters offer several advantages, including simple, cost-effective design, low sensitivity to water conductivity, and rapid measurement speed.[8] However, their accuracy declines in water-continuous emulsions, particularly when water content surpasses 50 vol% in light crude oils and

Department of Chemical & Petroleum Engineering, Schulich School of Engineering, University of Calgary, Calgary, Alberta T2N 1N4, Canada. E-mail: hhassanz@ucalgary.ca

© 2026 The Author(s). Published by the Royal Society of Chemistry

Open Access Article. Published on 27 May 2026. Downloaded on 5/30/2026 4:58:45 PM. This article is licensed under a Creative Commons Attribution-NonCommercial 3.0 Unported Licence.

80 vol% in heavy crude oils. Additionally, their performance can be affected by fluctuations in density, temperature, salinity, and the presence of gas bubbles.[7]

Tomography-based water-cut meters are used to generate 2D images of the cross-section of pipelines or vessels containing emulsions.[9] Several tomography techniques, such as gamma-ray, X-ray, electrical capacitance tomography (ECT), electrical resistance tomography (ERT), and electromagnetic tomography (EMT), can be used to produce cross-sectional images of the emulsion.[10] These images reveal the distribution of the water and oil phases within the emulsion.[11] Measurements using these methods can be taken multiple times at the same location, and they are non-invasive, meaning they do not interfere with the measured object. However, tomography-based water-cut meters have drawbacks, including the complexity and cost of the measuring instruments and their sensitivity to flow dynamics.

Gamma densitometry is a technique that utilizes the density difference between oil and water to measure the water content in emulsions.[12] It operates on the principle that gamma rays emitted by a radioactive source attenuate as they pass through materials of higher density. By measuring this attenuation, the emulsion density can be determined, allowing calculation of the water cut.[13] This technique is non-intrusive and capable of providing continuous, real-time measurements. However, it requires precise calibration and involves handling radioactive materials, posing safety concerns. Additionally, its accuracy can be affected by factors such as emulsion homogeneity, water salinity, and flow dynamics.[14]

Infrared water-cut meters utilize Near-Infrared (NIR) absorption spectroscopy to measure the water content in oil–water mixtures.[15] These meters exploit the significant difference in how crude oil and water absorb infrared radiation, particularly at specific wavelengths where water absorbs more energy than oil.[16] Infrared water-cut meters offer several advantages, including real-time measurement, a broad water-cut detection range (0–100%), and the ability to measure unaffected by water or oil density or water salinity variations. However, they also have some limitations, such as the need for periodic maintenance of the probe due to changes in its optical properties, the requirement for emulsion homogeneity, prior knowledge of the oil's absorption characteristics, and the necessity for inline validation testing to ensure measurement reliability.[8]

Coriolis flowmeters measure the mass flow rate and density of the bulk emulsion during the measurement process. These parameters, combined with the density of free oil and water, are used to calculate the volumetric flow rate and, subsequently, the water cut across the full range (0–100%) of water content in the emulsion.[17] For accurate water cut measurement, the density of the emulsion must lie between the density of free water (the upper limit) and the density of pure oil (the lower limit). However, the gas bubbles formed in the emulsion during the production process can reduce the emulsion's density, leading to an underestimation of the water cut value.[18]

Ultrasonic water-cut meters transmit ultrasonic waves through an oil–water mixture and measure their propagation through the emulsion. The speed of sound varies between oil and water, enabling the meter to determine the water cut across the full range (0–100%) of water content in the emulsion.[19] Key advantages of ultrasonic water-cut meters include ease of installation, minimal maintenance requirements, safety for personnel, the ability to penetrate highly dense emulsions, low cost, simple operation, and reduced sensitivity to temperature variations.[20,21] However, potential disadvantages include inaccuracies caused by gas bubbles or solid particles in the mixture, sensitivity to pressure variations, and the need for precise calibration to ensure reliable results.

Microwave sensors operate based on the principle that water and oil have significantly different dielectric constants. Water, being a polar molecule, has a high dielectric constant (around 80 at room temperature), while non-polar oil has a much lower dielectric constant (typically between 2 and 3 for bitumen).[22] Microwave sensors measure water cut by analyzing the interaction of microwave signals with the oil–water mixture, leveraging the difference in dielectric properties between oil and water.[23,24] They offer a reliable, non-invasive, real-time water cut measurement solution. However, they require careful calibration and are sensitive to factors like gas bubbles and temperature variations.

Conductivity meters operate on the significant difference in EC between brine, which contains ions (*e.g.*, Na^+, Cl^-), and crude oil, which has very low conductivity. This method relies on the principle that water, mainly when it contains dissolved salts (brine), is a good conductor, whereas oil is a poor conductor. By measuring the emulsion's electrical conductivity (or conductance), the water cut can be determined using Maxwell's equation, which correlates the emulsion's conductivities and the water's volume fraction of the continuous aqueous phase in the emulsion.[25] However, measuring water cut with conductivity meters requires a continuous water phase in the emulsion and has limitations, including dependence on water salinity, sensitivity to temperature variations, and susceptibility to gas interference.

While current water-cut measurement techniques, such as conventional tracer dilution, offer benefits such as real-time monitoring, they face significant practical hurdles in the petroleum industry. Most established methods rely on specialized tracers that require expensive equipment or struggle with crude oil's opacity. Furthermore, traditional offline methods require separating water from the entire bulk sample by distillation or large-scale centrifugation, which is energy-intensive and time-consuming.

In contrast, the proposed method only requires handling a small aliquot of the settled aqueous phase (typically less than 10 mL) for rapid measurement. This micro-scale approach avoids the logistical and environmental costs associated with treating the entire sample volume. Notably, there remains a lack of documented methods capable of providing accurate water-cut measurements for highly stable emulsions across the entire 0–100% range, particularly in complex processes such as Expanding Solvent Steam-Assisted Gravity Drainage (ES-SAGD).

This study aims to address this gap by introducing an offline full-range method that accurately determines water cut in production streams. The proposed approach leverages Boyle's

© 2026 The Author(s). Published by the Royal Society of Chemistry

Open Access Article. Published on 27 May 2026. Downloaded on 5/30/2026 4:58:45 PM.
This article is licensed under a Creative Commons Attribution-NonCommercial 3.0 Unported Licence.

law and salinity measurements to determine water cut. This developed measurement strategy offers several key advantages: applicability to whole samples without requiring fluid homogeneity, high accuracy across the entire range of water cut (0 to 100%), and the elimination of the need for water separation. Additionally, the method enhances efficiency, uses simple, cost-effective instruments, generates minimal waste, and requires low maintenance. It is also effective in challenging conditions, such as stable emulsions, high-salinity reservoirs, high-viscosity oils, water cuts near 100% or 1%, and scenarios with minimal density differences, while avoiding extensive data recording or processing. By overcoming the limitations of conventional techniques, this study provides a robust, reliable, and sustainable solution for water cut measurement in oil production operations.

2. Materials

Synthetic crude oil was prepared by diluting 60 wt% raw bitumen, characterized by a density of 1.01899 g cm^{-3} (7.24 ° API), with 40 wt% pure toluene (CAS #108-88-3). The resulting synthetic crude oil had a final density of 0.953552 g cm^{-3} and an API gravity of 16.76. Reverse osmosis (RO) water, with a conductivity of 90 mS cm^{-1}, was used as the aqueous phase. Sodium chloride (NaCl) (CAS #7647-14-5), with a purity of 99.99%, was purchased from VWR and added to the emulsions. The salinity of the brine, resulting from the dissolution of NaCl in the aqueous phase, was measured to determine the amount of water dispersed in the emulsion.

3. Experimental setups

3.1. Boyle's law measurement apparatus for the total volume of the emulsion

Traditional volumetric techniques are often susceptible to human error, thermal expansion, and measurement inconsistencies, all of which can significantly affect water-cut accuracy. This is particularly important for water-cut measurements at extreme water-cut levels. Leveraging Boyle's law provides a highly precise, repeatable, and robust method for emulsion volume measurement, ensuring that volumetric inaccuracies do not compromise water cut calculations. This approach eliminates common issues in traditional techniques and enhances confidence in water-fraction measurements. Accordingly, Boyle's law was utilized to precisely measure the total volume of emulsion, as illustrated in Fig. 1. The apparatus consists of an Ashcroft DG25 digital pressure gauge connected to the top of a 140 mL Swagelok double-ended stainless steel gas chamber. The pressure gauge provides readings to three decimal places with an accuracy of ±0.5% of full scale, up to 15 psig gauge pressure. At the bottom of the gas chamber, a 1/8-inch Swagelok three-way ball valve connects the chamber to both a nitrogen gas cylinder and an emulsion sampling bottle *via* flexible plastic tubes. Emulsion samples were stored in borosilicate glass bottles with volumes of 100 mL, 500 mL, and 1000 mL, each equipped with leak-proof GL 45 polypropylene caps. These glass bottles were chosen over plastic ones to prevent volume changes during measurement.

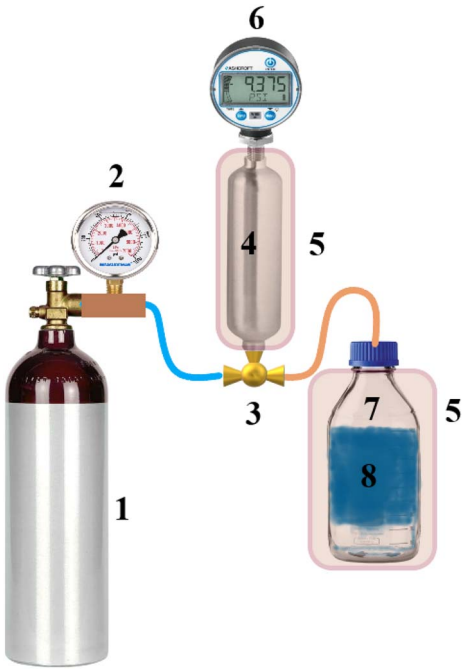

Fig. 1 Experimental setup for measuring the total volume of emulsion using Boyle's law. (1) Nitrogen cylinder, (2) gas pressure regulator, (3) 3-way valve, (4) stainless steel gas chamber, (5) glass wool thermal insulator, (6) high-accuracy digital pressure gauge, (7) borosilicate glass bottle, (8) sample emulsion.

The gas chamber and emulsion sampling bottle were insulated with glass wool to minimize temperature effects during measurement. Additionally, a Sartorius SECURA3102-1S high-accuracy digital balance, with a resolution of two decimal places and a maximum load capacity of 3 kg, was used to weigh both the empty and emulsion-filled bottles. It should be noted that the proposed method is intended for dead oil samples. To mitigate the potential impact of entrained gas or air bubbles on measurement accuracy, particularly in pressure-volume calculations and electrical conductivity, all emulsion samples were allowed to degas at atmospheric conditions in a fume hood before testing. This ensures that any gaseous phase is removed, preventing compressibility errors in the Boyle's law application and interference with the sensor–liquid interface during EC measurements. The high reproducibility of the volume results confirms that the impact of entrained gas under these conditions is negligible.

3.2. Measurement of brine salinity

The water content in the emulsion was determined by adding a specific weight of sodium chloride (NaCl). The mixture was thoroughly homogenized for 5 minutes at 15 000 rpm using a Polytron PT 2500 E mixer homogenizer. This process ensured that the salt was evenly distributed and reached all water droplets dispersed within the oil phase. The salinity of the aqueous phase was measured using multiple methods for

Open Access Article. Published on 27 May 2026. Downloaded on 5/30/2026 4:58:45 PM. This article is licensed under a Creative Commons Attribution-NonCommercial 3.0 Unported Licence.

comparison. These methods included refractive index, electrical conductivity, and gravimetric analysis, all of which were employed to ensure precise determination of the salinity. The measured salinity values, combined with the known weight of the added salt, were used to calculate the volume of water contained in the emulsion.

3.2.1. Brine salinity measurement using a refractometer. The Reichert Abbe Mark III digital refractometer (model: 1310488M) was used to measure the salinity of the brine at room temperature. The refractometer is equipped with six high-intensity LEDs for illumination and glass prisms to measure the refractive index (RI) within the range of 1.30000–1.70000 nD, with a readability of 0.00001 nD and an accuracy of ±0.00001 nD.[26] The instrument operates at the sodium D-line (589 nm) and can determine sugar concentrations in aqueous solutions over the range 0–95 wt% (Brix).

3.2.2. Brine salinity measurement using an electrical conductivity meter. The Mettler-Toledo SevenExcellence S470 pH/Conductivity Benchtop Meter, equipped with an InLab 731-ISM conductivity probe, was used to measure the electrical conductivity (EC) and, consequently, the salinity of the brine at room temperature. The conductivity meter can measure conductivity from 0.01 to 1000 mS cm^{-1}, with an accuracy of ±0.5% of full scale.[27]

3.2.3. Brine salinity measurement using the gravimetric method. The Ohaus Adventurer Pro AV264C balance was used to measure the weight of the brine and the remaining salt before and after the vaporization process, enabling the determination of brine salinity by the gravimetric method. The balance offers a readability of 0.0001 g, with a maximum capacity of 260 g during measurements. It also ensures linearity within ±0.0002 g.[28] The VWR 1400E vacuum oven was used to evaporate the brine's water and dry the remaining salt for salinity measurement. The vacuum oven can work at 40–200 °C with a temperature control of 0.2 °C.[29] The vacuum oven was operated at 100 °C and connected to a central vacuum system set at −20 in Hg during evaporation.

4. Experimental procedures

4.1. Volume measurement of known emulsion samples ($V_{emulsion}$)

A clean glass bottle with a volume of 500 mL was weighed empty using a digital balance and recorded as the weight of the clean bottle (W_{bottle} = 344.95 g). Seven different weight ratios (water cuts of 1, 5, 25, 50, 75, 95, and 99 wt%) of synthetic crude oil (40/60 wt% toluene/bitumen) were sequentially prepared in the same glass bottle by mixing synthetic crude oil with appropriate amounts of reverse osmosis (RO) water to produce 400 g of representative known emulsion samples (water-cut samples, WCS #1–#7). These samples were prepared to cover the full range of water cut measurements for low-viscosity synthetic crude oil.

Additionally, two known water-cut samples were prepared by mixing 100 g of pure bitumen with 300 g of RO water (WCS #8), and a 100 g mixture of 10/90 wt% toluene/bitumen with 300 g of RO water (WCS #9). These two samples were used to assess the accuracy of water-cut measurements for high-viscosity bitumen and heavy crude oils. Table 1 summarizes all known emulsion samples prepared for water cut measurements.

The weight of the clean bottle (W_{bottle}) was subtracted from the total weight of the bottle containing the emulsion (W_{total}) to obtain the weight of the emulsion ($W_{emulsion}$):

$$W_{emulsion}\,(g) = W_{total}\,(g) - W_{bottle}\,(g) \quad (1)$$

A thermally insulated gas chamber with a known volume ($V_{gas\ chamber}$ = 147.508 mL) was charged with nitrogen to approximately 18 psia absolute pressure. An accurate digital pressure gauge (with three decimal places) was connected to the top of the gas chamber to measure the pressure after charging ($P_{charging}$). The pressure gauge reading at atmospheric conditions (P_{offset}) was also recorded as an offset value. This offset pressure was subtracted from all pressure readings to ensure accurate measurements. Atmospheric pressure in the lab ($P_{atmospheric}$) was measured using an accurate barometer. The experiments showed that changes in atmospheric pressure did not affect the volume calculation. The gas chamber was connected to the sample bottle, and nitrogen was introduced into it. The equilibrium pressure ($P_{equliberim}$) after releasing nitrogen to sample bottle was measured. To eliminate temperature effects on the readings, the sample bottles were insulated. The free volume above the emulsion (V_{free}) was calculated using Boyle's law as follows:

$$V_{free}(mL) = V_{gas\ chamber}(mL) \times \frac{P_{charging}(psia) - P_{equilberium}(psia)}{P_{equilberium}(psia) - P_{atmospheric}(psia)} \quad (2)$$

The volume of the emulsion ($V_{emulsion}$) was then calculated as:

$$V_{emulsion}\,(mL) = V_{total}\,(mL) - V_{free}\,(mL) \quad (3)$$

It is worth mentioning that the total volume of the empty bottle (V_{total}) includes the volume of the bottle and the volume of the plastic tube connecting it to the three-way valve. This total volume was measured accurately using Boyle's law. To achieve this, first, a known weight of 400 g of RO water was charged into the glass bottle. The free volume above the water (V_{free}) was measured by obtaining Boyle's law parameters, as reported in eqn (2), and substituted into $V_{total} = V_{water} + V_{free}$ after converting the 400 g of water to V_{water} using the density of water. The total volume of the empty bottle was then determined and recorded as V_{total} = 613.65 mL.

4.2. Measurement of brine salinity (C_{NaCl}) for known emulsion samples

To determine the amount of water dispersed in the known emulsion samples, the weight of sodium chloride (W_{NaCl}) and the mass concentration of salt (C_{NaCl}), referred to as brine salinity, must be measured accurately. The brine salinity for the known emulsion samples was measured using three different techniques: RI, EC, and gravimetry. The results from these

© 2026 The Author(s). Published by the Royal Society of Chemistry

Open Access Article. Published on 27 May 2026. Downloaded on 5/30/2026 4:58:45 PM. This article is licensed under a Creative Commons Attribution-NonCommercial 3.0 Unported Licence.

Table 1 Weights of RO water and synthetic crude oil used for preparing known emulsion samples across the full range of water cut measurements

Sample name	S#	Emulsion	W_{NaCl}	W_{water}	W_{oil}	$W_{emulsion}$	WC (w/w)
WCS	1	RO-40/60[a]	16.1820	396.08	3.93	400.01	0.99
	2		15.2549	380.02	20.05	400.07	0.95
	3		12.1733	300.02	100.04	400.06	0.75
	4		8.1121	200.00	200.00	400.00	0.50
	5		3.9650	100.00	300.02	400.02	0.25
	6[d]		4.7558	20.01	380.04	400.05	0.05
	7[d]		4.0211	4.02	396.10	400.12	0.01
	8[e]	RO-100[b]	11.7151	300.04	100.01	400.05	0.75
	9[e]	RO-10/90[c]	11.7167	299.99	100.40	400.39	0.75

[a] Oleic phase is 40/60 wt% toluene/bitumen. [b] Oleic phase is 100 wt% bitumen. [c] Oleic phase is 90/10 wt% toluene/bitumen. [d] For samples WCS #6 and WCS #7, 100 g of RO water was added to the emulsion sample after measuring its volume to facilitate representative aqueous sampling. [e] For samples WCS #8 and WCS #9, 100 g of toluene was added to the emulsion sample after measuring its volume to reduce the viscosity and IFT of the oleic phase and enable salt to reach all water droplets in the water-in-oil emulsion.

methods were compared with the actual known brine salinity values to evaluate each technique's accuracy. Both the RI and EC methods require a calibration curve relating brine salinity to the corresponding measurement parameter (RI or EC) before determining the brine salinity of the known emulsion samples.

To implement these techniques, three calibration samples (brine-salinity calibration samples, (BSCS #1–#3) were prepared by mixing 30 g of RO water with 10 g of synthetic crude oil (40/60 wt% toluene/bitumen) to create oil-in-water emulsions. Different weights of NaCl were added to these three prepared calibration samples to generate calibration samples with varying mass concentrations of NaCl in water, as shown in Table 2. It is important to note that the same crude oil should first be mixed with water to create an emulsion in the calibration samples before adding NaCl. This ensures the creation of a representative brine and an accurate calibration curve.

For actual samples containing oil mixed with formation brine (rather than freshwater), the formation brine should be used as the base when establishing the calibration curve to account for its initial salinity.

In field applications where brine salinity is extremely high, such as in certain shale formations, the linear relationship between brine salinity and RI and EC may no longer hold. To maintain measurement accuracy under these conditions, a reverse calibration approach can be employed. Instead of increasing the salt concentration (which could push the system further outside the linear range), controlled amounts of distilled water are added to the brine to dilute it and bring the brine into the linear region of the RI or EC response curve. This requires separating the brine phase from the emulsion *via* centrifugation, then systematically diluting and measuring RI or EC for each diluted sample. A calibration curve can then be constructed based on the diluted samples, allowing accurate back-calculation of the original high salinity. This strategy extends the method's applicability to highly saline systems, ensuring reliable water-cut measurements across a broader range of field conditions.

The RI and EC of the calibration samples were measured and correlated with the mass concentration of NaCl (C_{NaCl}) in brine to generate calibration curves for the RI and EC techniques.

4.2.1. Development of a salinity–RI calibration curve for known emulsion samples. To evaluate the salinity of brine in known emulsion samples (WCS #1–#9, Table 1), a calibration curve correlating brine salinity with the RI of prepared calibration samples (BSCS #1–#3, Table 2) was first established. A few droplets of the oil-free brine from each calibration sample were placed on the digital refractometer, and the RI was measured three times for repeatability. Notably, the refractometer provides consistent, repeatable values after a few initial readings; hence, error bars cannot be generated for the RI measurements due to their negligible variability. Consequently, the repeatable RI values were plotted against the mass concentration of NaCl for the calibration samples, as shown in Fig. 2(a).

It is worth noting that the linearity of the calibration curves for both RI and EC was initially confirmed through a multi-point analysis ($R^2 > 0.99$); based on this pre-validated linear regime, a three-point calibration protocol was subsequently adopted for routine measurements to ensure both accuracy and efficiency. With the three-point calibration protocol, the RI shows a linear relationship with brine salinity, expressed as the mass concentration of NaCl per liter of brine, as a function of

Table 2 Weights of NaCl and volumes of brine used for generating salinity–RI and salinity–EC calibration curves for known emulsion samples

BSCS#	W_{NaCl} (g)	V_{brine} (L)	C_{NaCl} (g_{NaCl} L_{brine}^{-1})	Average RI (nD)	Average EC (μS m^{-1})
1	0.6071	0.030402	19.9694	1.33664	335.06
2	1.2251	0.030653	39.9670	1.33996	624.14
3	1.8041	0.030940	58.3088	1.34295	869.58

Open Access Article. Published on 27 May 2026. Downloaded on 5/30/2026 4:58:45 PM.
This article is licensed under a Creative Commons Attribution-NonCommercial 3.0 Unported Licence.

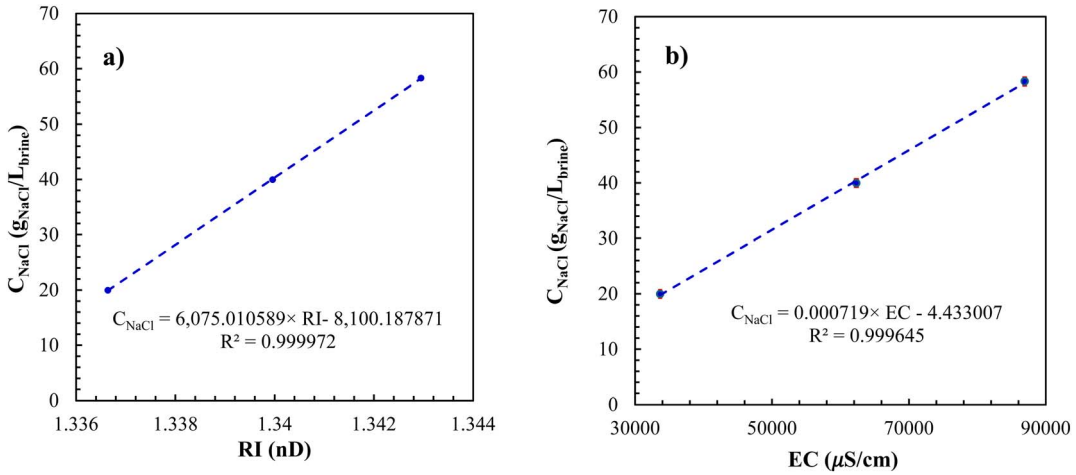

Fig. 2 (a) Salinity–RI calibration curve, (b) salinity–EC calibration curve for known emulsion samples.

RI. The brine salinity for the known emulsion samples is then determined using the salinity–RI calibration correlation as follows:

$$C_{NaCl}\,(g_{NaCl}\,L_{brine}^{-1}) = a_{RI} \times RI + b_{RI} \quad (4)$$

where $a_{RI} = 6075.010589$ and $b_{RI} = -8100.187871$.

4.2.2. Development of a salinity–EC calibration curve for known emulsion samples. The EC of the oil-free brine extracted from the prepared calibration samples (BSCS #1–#3, Table 2) was measured six times per sample to ensure accuracy and repeatability. The standard deviations of the six readings for each calibration sample were small relative to the arithmetic average, making the error bars (red lines) visually hidden behind the markers (blue circles), as shown in Fig. 2(b). The arithmetic average of the EC values was plotted against the brine salinity of the calibration samples. The results demonstrate a linear relationship between EC and brine salinity, as shown in Table 2 and Fig. 2(b). This calibration curve was then used to determine the brine salinity for the known emulsion samples using the following equation:

$$C_{NaCl}\,(g_{NaCl}\,L_{brine}^{-1}) = a_{EC} \times EC\ (\mu m\ cm^{-1}) + b_{EC} \quad (5)$$

where $a_{EC} = 0.000719$ and $b_{EC} = -4.433007$.

4.2.3. Brine salinity measurement using gravimetry. The gravimetric method offers the advantage of measuring brine salinity without requiring a calibration curve. Approximately 5 grams of representative oil-free brine was extracted from each known emulsion sample (WCS #1–#9, Table 1). The water was then evaporated, leaving behind a solid residue that directly provides the mass concentration of NaCl in the brine, as calculated using the following equation:

$$C_{NaCl}(g_{NaCl}\,L_{brine}^{-1}) = \frac{W_{NaCl}\ (g)}{V_{brine}(L)} = \frac{W_{NaCl}}{\frac{W_{NaCl}}{\rho_{NaCl}} + \frac{W_{water}}{\rho_{water}}} \quad (6)$$

where W_{NaCl} is the weight of NaCl (in grams) in the brine, V_{brine} is the volume of brine (in liters), ρ_{NaCl} and ρ_{water} are the densities of NaCl and water (in g cm^{-3}), respectively. To ensure the removal of all oleic contaminants, the samples were filtered using a 0.22 micrometer Nylon syringe filter. The filtered samples were placed in open 50 mL plastic centrifugal tubes and left in a vacuum oven under a vacuum pressure of −20 inches of mercury at 100 °C for two days to ensure complete water evaporation from the NaCl. The weights of the samples were recorded before and after evaporation to determine the brine salinity *via* gravimetry. SI Tables A-3–A-5 and Fig. 6–8 show the results obtained from the gravimetric method and compare them with those from the RI and EC techniques.

After measuring the brine salinity using RI, EC, and gravimetry techniques, the volume of water dispersed in the emulsion, and consequently the water cut, can be easily determined for known emulsion samples. This is achieved by using the known weight of NaCl added to the emulsion, as brine salinity is defined as the weight of NaCl per unit volume of water.

4.3. Water cut measurement for known emulsion samples

After measuring the volume of known emulsion samples (WCS #1–#9) using Boyle's law, a specific amount of NaCl was added to each tested emulsion sample, as shown in Table 1. The emulsion was then homogenized at 15 000 rpm for 10 minutes to ensure that the salt reached all water droplets dispersed throughout the emulsion. The emulsion was left to settle for some time, and approximately 30 mL of the separated aqueous phase was centrifuged at 6000 rpm for 3 minutes to obtain an oil-free brine sample.

For known emulsion samples with low water content (WCS #6 (5 wt% water cut) and WCS #7 (1 wt% water cut)), it is challenging for the salt to reach all water droplets dispersed in the oleic phase. Additionally, extracting representative brine samples for RI or EC measurement becomes difficult. To address this issue, a fixed volume of water (100 mL) was added to each low-water-content sample to increase the water content. This added volume was later subtracted from the final water content of the crude oil.

The high viscosity and interfacial tension associated with bitumen and heavy crude oils further restrict the accessibility of

© 2026 The Author(s). Published by the Royal Society of Chemistry

Open Access Article. Published on 27 May 2026. Downloaded on 5/30/2026 4:58:45 PM. This article is licensed under a Creative Commons Attribution-NonCommercial 3.0 Unported Licence.

salt to water droplets dispersed in the oleic phase. To overcome this challenge, a proportional amount of viscosity-reducing solvent (100 mL of toluene) was added to the high-viscosity known emulsion samples (WCS #8 and #9) after measuring the volume of the tested emulsion sample using Boyle's law. It is worth noting that adding toluene to the tested emulsion sample after measuring its volume enhances the accessibility of salt to water droplets without affecting the water cut calculations. It is important to note that the proposed method is specifically designed for the stable emulsions encountered in petroleum recovery. The robustness of this technique was validated within the context of asphaltene-stabilized interfaces and high-viscosity oils. For exceptionally stable emulsions where rigid interfacial films limit mass transfer, adding a few drops of a commercial demulsifier (*e.g.*, DMO46X) is recommended to help break the emulsion. Because these chemical agents partition into the oleic phase, they do not affect the RI or EC of the separated aqueous phase. While other specialized systems, such as Pickering emulsions, present different challenges, they fall outside the current scope of this study and remain an area for future investigation.

The RI and EC of each tested known emulsion sample were measured multiple times to ensure repeatability. The RI or EC values were then substituted into the previously established linear calibration curves to determine the brine salinity for the tested known emulsion samples. Once the mass concentration of salt in the brine (C_{NaCl}) and the weight of added NaCl (W_{NaCl}) are known, the volume of brine (V_{brine}) is calculated as follows:

$$V_{\mathrm{brine}}(\mathrm{mL}) = \frac{W_{\mathrm{NaCl}}(\mathrm{g})}{C_{\mathrm{NaCl}}\left(\mathrm{g_{NaCl}\ L_{brine}^{-1}}\right)} \times 1000 \tag{7}$$

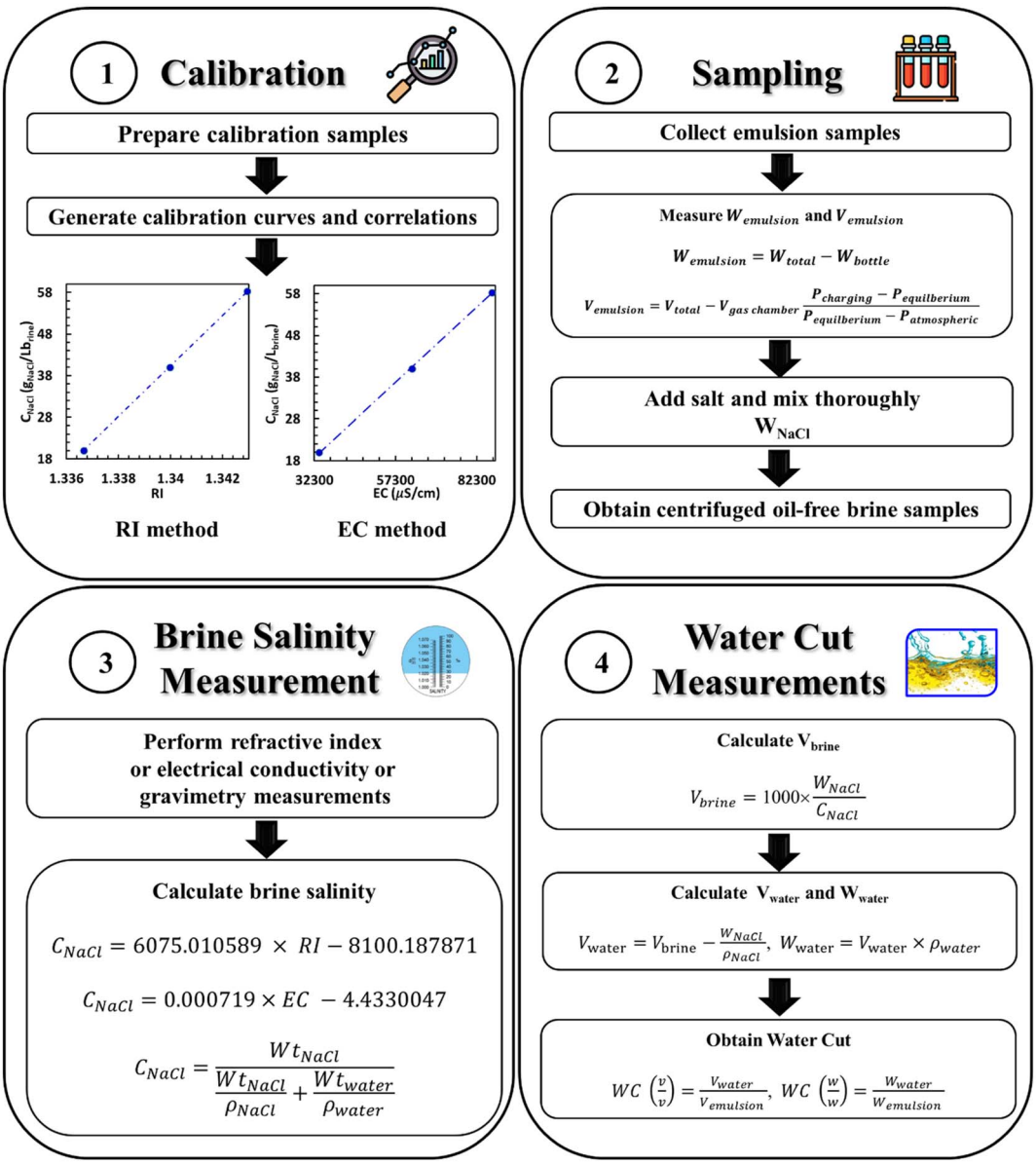

Fig. 3 Steps followed toperform water cut measurements.

Open Access Article. Published on 27 May 2026. Downloaded on 5/30/2026 4:58:45 PM.
This article is licensed under a Creative Commons Attribution-NonCommercial 3.0 Unported Licence.

The volume of water present in the brine was obtained by subtracting the volume of added salt:

$$V_{\text{water}}(\text{mL}) = V_{\text{brine}}(\text{mL}) - \frac{W_{\text{NaCl}}(\text{g})}{\rho_{\text{NaCl}}\ (\text{g mL}^{-1})} \quad (8)$$

The weight of water (W_{water}) was then calculated as:

$$W_{\text{water}}\ (\text{g}) = \rho_{\text{water}}\ (\text{g mL}^{-1}) \times V_{\text{water}}\ (\text{mL}) \quad (9)$$

where ρ_{w} g mL^{-1} is the water density before adding the salt to the sample. The water cut as a volume fraction (v/v) was obtained by dividing the measured water volume (V_{water}) by the total volume of the emulsion sample (V_{emulsion}), which was determined using Boyle's law:

$$\text{WC(v/v)} = \frac{V_{\text{water}}(\text{mL})}{V_{\text{emulsion}}(\text{mL})} \quad (10)$$

To calculate the water cut as a weight fraction (w/w), the measured weight of water (W_{water}) was divided by the total weight of the emulsion sample (W_{emulsion}), which was measured using a balance:

$$\text{WC(w/w)} = \frac{W_{\text{water}}(\text{g})}{W_{\text{emulsion}}(\text{g})} \quad (11)$$

Fig. 3 summarizes the steps for obtaining water cut measurements in the known emulsion samples.

5. Results and discussion

5.1. Accuracy of Boyle's law for liquid volume measurements

To assess the accuracy of the Boyle's law technique used in this study for measuring liquid volumes in different VWR bottles, three glass bottles of varying sizes (100 mL, 500 mL, and 1000 mL) were selected. Each bottle was filled with a specific mass of RO water (80.09 g, 400.15 g, and 800.02 g). Using the density of RO water, these masses were converted into their actual volumes: 80.232 mL, 400.862 mL, and 801.443 mL, respectively. The parameters required for Boyle's law were measured three times for repeatability and applied to eqn (2) and (3) to calculate the volume of water in each bottle. Table 3 presents Boyle's law parameters and the liquid volumes obtained using this technique.

The volume of the same mass of water contained in each bottle was measured again using two additional methods: the volumetric method and the fill-to-full liquid method. These measurements were performed to compare the accuracy of these methods and the Boyle's law technique relative to the actual volume of water, determined from the water's mass.

In the volumetric method, an accurate graduated glass tube (25 mL) was used to measure the total volume of water in each bottle. In the fill-to-full method, the total volume of each bottle was first measured by filling it with RO water and converting the water mass to volume using the water density. Subsequently, the same weight of RO water (80.09 g, 400.15 g, or 800.02 g) was added to the empty, dry bottle, and the bottle was refilled to the brim with RO water. The volume of the added water was subtracted from the bottle's total volume to determine the volume of the sample water.

SI Table A-1 and Fig. 4 present the results of measuring water volumes using the three methods and compare them with the actual water volume. The Average Absolute Relative Deviation Percentage (AARD%) for each method was calculated relative to the actual volume of water using the following formula:

$$\text{AARD\%} = \frac{100}{N}\sum_{i=1}^{N}\frac{\text{Avg. } V_{\text{water}}^{\text{measured},i} - V_{\text{water}}^{\text{actual},i}}{V_{\text{water}}^{\text{actual},i}} \quad (12)$$

where N is the number of samples, (Avg. $V_{\text{water}}^{\text{measured},i}$) is the average volume of water measured by the method for the i-th sample, and ($V_{\text{water}}^{\text{actual},i}$) is the actual volume of water for the i-th sample.

The results demonstrate that the volumetric method had the lowest accuracy among the evaluated techniques. However, the measurement error associated with this method was still small and decreased as the water volume in the bottle increased. This trend can be attributed to the influence of tubing wettability, which causes minor water droplets to adhere to the inner walls of the measuring tube during the measurement process. As illustrated in SI Table A-1, the relative impact of these adhesive forces diminishes with larger volumes as the proportion of water lost to droplet retention becomes less significant. Consequently, the volumetric method demonstrates improved accuracy at higher volumes, where the error introduced by wettability effects is reduced.

Boyle's law technique for volume measurement demonstrated the highest accuracy for all bottle sizes, reflecting its

Table 3 Boyle's law parameters and measured water volumes

Bottle size	P_{charging} (psia)	$P_{\text{equliberium}}$ (psia)	V_{free} (mL)	V_{water} (mL)	Avg. V_{water} (mL)
100 mL	15.881	15.143	48.534	80.339	80.275
	15.925	15.175	48.629	80.244	
	15.929	15.178	48.630	80.243	
500 mL	18.341	15.128	212.721	400.928	400.862
	18.286	15.105	212.800	400.849	
	18.399	15.151	212.841	400.808	
1000 mL	20.222	15.181	325.992	801.361	801.199
	20.862	15.379	326.255	801.098	
	19.991	15.108	326.215	801.139	

© 2026 The Author(s). Published by the Royal Society of Chemistry

Open Access Article. Published on 27 May 2026. Downloaded on 5/30/2026 4:58:45 PM.
This article is licensed under a Creative Commons Attribution-NonCommercial 3.0 Unported Licence.

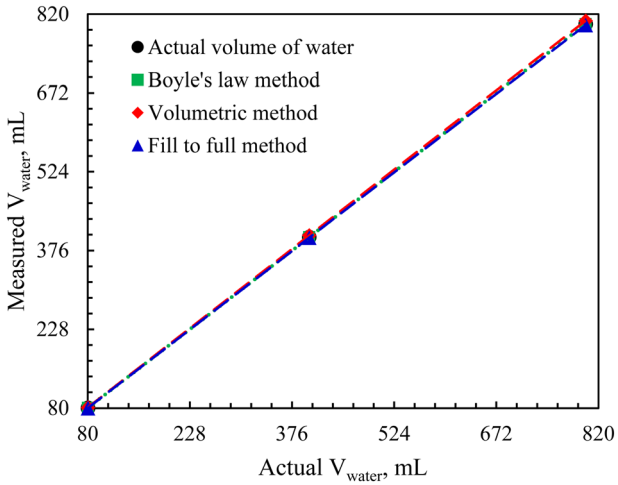

Fig. 4 Measured *versus* actual volume of water (black circles) using three techniques: (1) Boyle's law technique (green squares), (2) volumetric technique (red diamonds), and (3) fill to full of liquid technique (blue triangles).

ability to measure volumes accurately regardless of bottle size. The total error (∑AARD%) for the Boyle's law technique was 0.028, compared to 0.84 and 0.26 for the volumetric and fill-to-full methods, respectively, across the three glass bottles, as shown in SI Table A-1. The emulsion volume was determined using Boyle's law, assuming the isothermal expansion of nitrogen. This approach is thermodynamically consistent for our setup, as nitrogen behaves nearly ideally at the operating pressure (approx. 10 psi) and room temperature, with a compressibility factor (Z) of approximately 1.0. To ensure isothermal conditions, measurements were taken only after thermal equilibrium was established between the nitrogen cylinder and the room temperature. The accuracy of this method was experimentally validated by measuring known volumes of water, yielding results in excellent agreement with the actual values, confirming the robustness of the pressure–volume relationship in this application.

It is worth noting that the fill-to-full method exhibits minor measurement errors compared to the Boyle's law technique, primarily due to difficulties in repeating measurements and in identifying the same endpoint during bottle filling. Furthermore, tiny air bubbles adhere to the bottle walls due to surface tension and wettability forces, thereby increasing measurement errors. Another drawback of the fill-to-full method compared to the Boyle's law method is that no space is left for adding salt or toluene when the bottle is full of water, making it impractical for certain applications. Unlike the volumetric or fill-to-full methods, using gases for volume measurement *via* Boyle's law is more accurate because it avoids surface tension and wettability issues that hinder repeatability. Additionally, gases can readily access all spaces above the material, even if the material has an irregular surface, ensuring more reliable measurements.

5.2. Volume measurement for known emulsion samples

The volumes of known emulsion samples (WCS #1–#9, Table 1) were measured three times using the Boyle's law technique, as described in eqn (2) and (3). The arithmetic average of the measured volumes was plotted against the ideal volumes of the known emulsion samples, as shown in Fig. 5. The ideal volume of the emulsion was calculated by adding the division of the mass of the water and oil by their respective densities, as follows:

$$\text{Ideal } V_{\text{emulsion}}(\text{mL}) = \frac{W_{\text{water}}\ (\text{g})}{\rho_{\text{water}}\left(\text{g mL}^{-1}\right)} + \frac{W_{\text{oil}}\ (\text{g})}{\rho_{\text{oil}}\left(\text{g mL}^{-1}\right)} \quad (13)$$

The average absolute relative deviation percent error (AARD%) of measured volumes was calculated relative to the ideal volume of the emulsion. The results demonstrate excellent agreement between the average measured and ideal volumes of the emulsions, with a total error (∑AARD%) of 0.153 for all prepared known emulsion samples, as shown in SI Table A-2 and Fig. 5.

5.3. Brine salinity measurement for known emulsion samples

The brine salinity, expressed as the mass concentration of NaCl per liter of brine, of known emulsion samples (WCS #1–#9, Table 1) was measured and calculated using eqn (4)–(6) using three techniques: RI, EC, and gravimetry. The results are presented in Tables 4 and 5. The brine salinity data from Tables 4 and 5 were then substituted into eqn (7) and (8) to determine the water volumes in the emulsions for each method. The average absolute relative deviation percent error (AARD%) of the water volumes obtained using these methods was calculated relative to the actual water volume of each known emulsion sample, as shown in SI Table A-3. These calculated water volumes were compared and plotted against the actual water volumes, as shown in Fig. 6.

The results indicate that the RI and EC techniques are the most accurate methods for measuring water volume in emulsions, with total errors (∑AARD%) of 1.702 and 2.819, respectively, across all known emulsion samples. In contrast, the

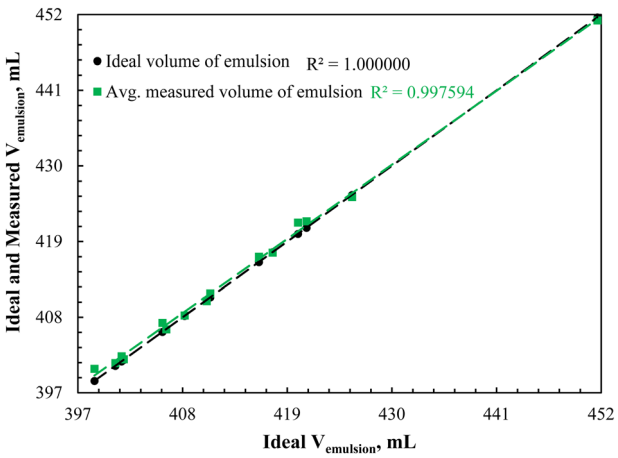

Fig. 5 Arithmetic average of volumes measured using Boyle's law technique (green squares) *versus* ideal volumes (black circles) for known emulsion samples.

Open Access Article. Published on 27 May 2026. Downloaded on 5/30/2026 4:58:45 PM. This article is licensed under a Creative Commons Attribution-NonCommercial 3.0 Unported Licence.

Table 4 Brine salinity measured using RI and EC techniques for known emulsion samples prepared for water cut measurements

Sample name	S#	Emulsion	WC (w/w)	W_{NaCl} (g)	Avg. RI (nD)	C_{NaCl} from RI (g_{NaCl} L_{brine}^{-1})	Avg. EC (μS cm^{-1})	C_{NaCl} from EC (g_{NaCl} L_{brine}^{-1})
WCS	1	RO- 40/60[a]	0.99	16.1820	1.33991	39.78	62 277	40.36
	2		0.95	15.2549	1.33983	39.29	61 454	39.77
	3		0.75	12.1733	1.3399	39.72	62 599	40.59
	4		0.50	8.1121	1.34	40.33	62 876	40.79
	5		0.25	3.9650	1.33973	38.69	61 401	39.73
	6[d]		0.05	4.7558	1.3397	38.50	60 555	39.12
	7[d]		0.01	4.0211	1.33956	37.65	59 363	38.27
	8[e]	RO-100[b]	0.75	11.7151	1.33967	38.32	60 481	39.07
	9[e]	RO-10/90[c]	0.75	11.7167	1.33967	38.32	60 354	38.98

[a] Oleic phase is 40/60 wt% toluene/bitumen. [b] Oleic phase is 100 wt% bitumen. [c] Oleic phase is 90/10 wt% toluene/bitumen. [d] For samples WCS #6 and WCS #7, 100 g of RO water was added to the emulsion sample after measuring its volume to facilitate representative aqueous sampling. [e] For samples WCS #8 and WCS #9, 100 g of toluene was added to the emulsion sample after measuring its volume to reduce the viscosity of the oleic phase and enable salt to reach all water droplets in the water-in-oil emulsion.

Table 5 Brine salinity measured using the gravimetry technique for known emulsion samples prepared for water cut measurement

Sample name	S#	Emulsion	WC (w/w)	W_{brine} (g)	W_{NaCl} (g)	W_{water} evaporated by gravimetry (g)	W_{water} in the emulsion sample (g)	C_{NaCl} from gravimetry (g_{NaCl} L_{brine}^{-1})
WCS	1	RO-40/60[a]	0.99	5.0719	16.1820	4.8772	405.356	39.131
	2		0.95	5.3516	15.2549	5.1472	384.149	38.929
	3		0.75	5.1108	12.1733	4.9126	301.728	39.540
	4		0.50	5.3376	8.1121	5.1309	201.366	39.482
	5		0.25	5.629	3.9650	5.4172	101.413	38.339
	6[d]		0.05	5.5849	4.7558	5.3742	21.293	38.443
	7[d]		0.01	5.3582	4.0211	5.161	5.198	37.483
	8[e]	RO-100[b]	0.75	5.1699	11.7151	4.9773	302.750	37.951
	9[e]	RO-10/90[c]	0.75	5.175	11.7167	4.9797	298.749	38.456

[a] Oleic phase is 40/60 wt% toluene/bitumen. [b] Oleic phase is 100 wt% bitumen. [c] Oleic phase is 90/10 wt% toluene/bitumen. [d] For samples WCS #6 and WCS #7, 100 g of RO water was added to the emulsion sample after measuring its volume to facilitate representative aqueous sampling. [e] For samples WCS #8 and WCS #9, 100 g of toluene was added to the emulsion sample after measuring its volume to reduce the viscosity of the oleic phase and enable the salt to reach all water droplets in the water-in-oil emulsion.

gravimetry technique exhibits a slight deviation, particularly at higher water volumes in the emulsion, with a total error (∑AARD%) of 2.871, as shown in Fig. 6 and SI Table A-3. The higher error associated with the gravimetric method can be attributed to the sensitivity of the analytical balance (readable to four decimal places). In particular, achieving consistent, repeatable measurements to the final two decimal places is challenging, which contributes to greater experimental uncertainty. In contrast, the digital refractometer and electrical conductivity meter provide higher repeatability than the gravimetric balance used in the gravimetry technique.

5.4. Water cuts measurement for known emulsion samples

The volumes and masses of water obtained from brine salinity measurement techniques were applied in eqn (10) and (11) to calculate the volumetric water cut (v/v) and mass water cut (w/w), respectively, for all known emulsion samples (WCS #1–#9, Table 1). The average absolute relative deviation (AARD%) was calculated for measured volumetric (v/v) and mass water cuts (w/w) relative to the actual water cuts. The actual volumetric water cut (v/v) for the known emulsion samples was calculated by dividing the actual RO water volume obtained from water density by the ideal volume of emulsion, while the actual mass water cut (w/w) was calculated by dividing the actual RO water weight by the emulsion weight measured using a balance.

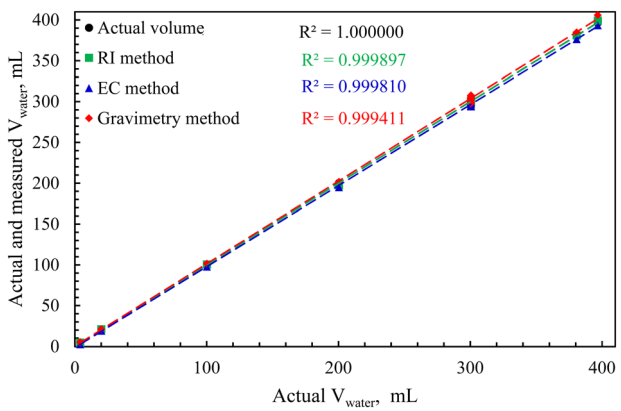

Fig. 6 Measured *versus* actual volumes (black circles) of water in known emulsion samples using three techniques: (1) RI (green squares), (2) EC (blue triangles), and (3) gravimetry (red diamonds).

© 2026 The Author(s). Published by the Royal Society of Chemistry

Open Access Article. Published on 27 May 2026. Downloaded on 5/30/2026 4:58:45 PM.
This article is licensed under a Creative Commons Attribution-NonCommercial 3.0 Unported Licence.

Both volumetric (v/v) and mass water cut (w/w) results demonstrate the superiority of the RI method, with total errors (∑AARD%) of 1.695 and 1.711, respectively, compared to 2.945 and 2.809 for the EC method and 2.747 and 2.874 for the gravimetry method. Although the EC and gravimetry methods exhibit slightly higher errors, they remain reliable techniques for measuring water cut. These results are summarized in SI Tables A-4 and A-5.

Adding 100 g of RO water to low water-content emulsion samples (sample WCS #6: WC = 0.05, and WCS #7: WC = 0.01) and subtracting it during the final water content calculation significantly improved the accuracy of volumetric (v/v) and mass water cut (w/w) measurements for all techniques. This confirms the effectiveness of this approach in overcoming challenges associated with spreading salt and collecting representative samples when the water content is low. Furthermore, adding 100 g of toluene to the viscous emulsion samples (samples WCS #8 and WCS #9) improved the accuracy of volumetric (v/v) and mass water cut (w/w) measurements for all three techniques (RI, EC, and gravimetry). This addition mitigated the resistance caused by the high viscosity of the oleic phase, enabling better salt distribution in the dispersed water droplets.

The obtained volumetric (v/v) and mass water cut (w/w) were plotted against the actual water cuts of known emulsion samples, as shown in Fig. 7 and 8, respectively. The volumetric (v/v) and mass water cut (w/w) values obtained using the RI, EC, and gravimetry techniques showed excellent agreement across the entire range of actual water cut values.

5.5. Water cut measurement for unknown actual emulsion samples

After assessing the accuracy of RI and EC techniques for measuring water cut in known emulsion samples (WCS #1–#9, Table 1), we applied these methods to determine the water cut of unknown emulsion samples. These samples were collected from a 3D physical model of Steam-Assisted Gravity Drainage (SAGD) conducted in our laboratory to mimic the field-produced emulsion.

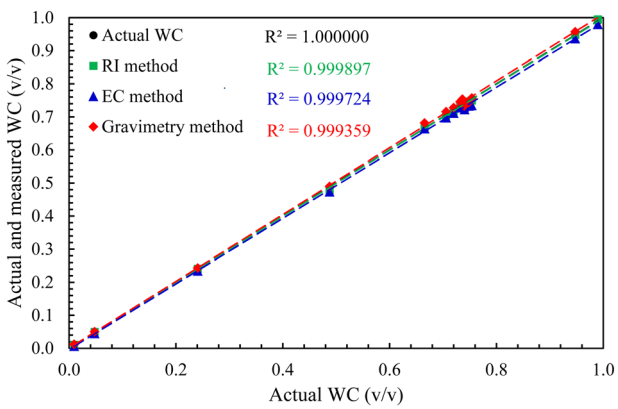

Fig. 7 Measured *versus* actual volumetric water cut (v/v) (black circles) of known emulsion samples using three techniques: (1) RI (green squares), (2) EC (blue triangles), and (3) gravimetry (red diamonds).

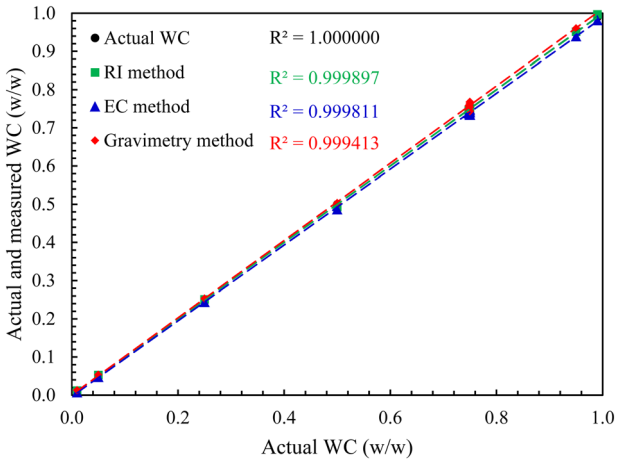

Fig. 8 Measured *versus* actual mass water cuts (w/w) (black circles) of known emulsion samples using three techniques: (1) RI (green squares), (2) EC (blue triangles), and (3) gravimetry (red diamonds).

The produced emulsion was collected in 24 glass bottles, each containing approximately 800 mL of emulsion. The weight (W_{bottle}) and total volume (V_{total}) of empty glass bottles were measured and recorded before collecting the emulsion samples. Unlike emulsions composed of conventional crude oil and brine, which typically separate under gravity, the SAGD process emulsions exhibited high stability, with bitumen and water remaining mixed for extended periods without separation.

To determine the coefficients a_{RI} and b_{RI} for eqn (4), which relates RI to salinity, two groups of calibration samples (RI calibration samples, RICS #1–#8) were prepared. Each calibration sample was prepared by taking 10 mL of the aqueous phase from each of four unknown emulsion samples (UES #1–#4). Sodium chloride was added to the calibration samples: 0.3 g was added to the first group (RICS #1, #3, #5, #7), and 0.6 g was added to the second group (RICS #2, #4, #6, #8).

To enhance the separation of any remaining oil from the aqueous phase, 2 mL of toluene was added to each calibration sample (RICS #1–#8), followed by centrifugation at 6000 rpm for 3 minutes. Toluene addition is essential, as the extracted water may contain micro- or nano-sized oil particles, and the added toluene is highly effective at extracting these particles into the oleic phase. This process yielded clear brine samples suitable for calibration. The RI of the extracted brine was measured three times, and the arithmetic average was plotted against brine salinity to derive the calibration coefficients, as presented in SI Table A-6.

The RI measurements of the brine-salinity calibration samples derived from different unknown samples (UES #1–#4) exhibited a perfectly linear trend. This confirms that all unknown samples (UES #1–#24) share the same calibration curve, with identical slope (a_{RI}) and intercept (b_{RI}) values. Fig. 9(a) illustrates the linear calibration, with coefficients a_{RI} = 6088.742153 and b_{RI} = −8119.354491.

To determine the EC coefficients a_{EC} and b_{EC} for eqn (5), which relates EC to brine salinity, four calibration samples (EC

Open Access Article. Published on 27 May 2026. Downloaded on 5/30/2026 4:58:45 PM. This article is licensed under a Creative Commons Attribution-NonCommercial 3.0 Unported Licence.

calibration samples, ECCS #1–#4) were prepared. Each calibration sample consisted of a 35 mL aqueous phase taken from the final collected unknown emulsion sample (UES #24). Sodium chloride was added to three of the samples: 1 g of NaCl to the second sample (ECCS #2), 2 g to the third sample (ECCS #3), and 3 g to the fourth sample (ECCS #4), while the first sample (ECCS #1) remained free of NaCl. To separate the remaining oil from the aqueous phase and obtain clear brine, 5 mL of toluene was added to each calibration sample, followed by centrifugation at 6000 rpm for 3 minutes. The EC of each sample was measured six times, and the arithmetic average was plotted against the mass concentration of NaCl in the brine to derive the calibration coefficients, as summarized in SI Table A-7. Notably, the error bars for the calibration samples (ECCS #1–#4) were negligible. Fig. 9(b) displays the linear calibration curve for EC, with coefficients $a_{EC} = 0.000725$ and $b_{EC} = -1.954176$.

To measure the water cut in 24 unknown emulsion samples, the volume of emulsion in each sample was first measured three times using Boyle's law technique, and the arithmetic average was recorded, as shown in SI Table A-8. Approximately 35 g of NaCl and 100 mL of toluene were then added to each sample to reduce oil viscosity and facilitate the dispersion of NaCl throughout the emulsion, ensuring it reached all dispersed water droplets. The mixture was homogenized at 15 000 rpm for 10 minutes to achieve uniform distribution of the salt in the aqueous phase. A 30 mL sample was subsequently collected from the bottom of each glass bottle and centrifuged at 6000 rpm for 3 minutes to obtain clear brine. The RI and EC of the extracted brine were measured multiple times for each unknown emulsion sample. The arithmetic averages of these measurements were substituted into eqn (4) and (5) to determine the brine salinity. The calculated brine salinity was then used in eqn (7) and (8) to compute the water volume, as presented in . Additionally, the aqueous phase of the unknown emulsion samples was separated using a centrifuge after adding a demulsifier (DMO46X) to improve water separation from the oleic phase. The water volume obtained from the centrifuge method was used for comparison with the values derived from the RI and EC methods.

The volumetric water cut ($WC_{,i}$) (v/v) for each unknown emulsion sample was calculated using the following equation:

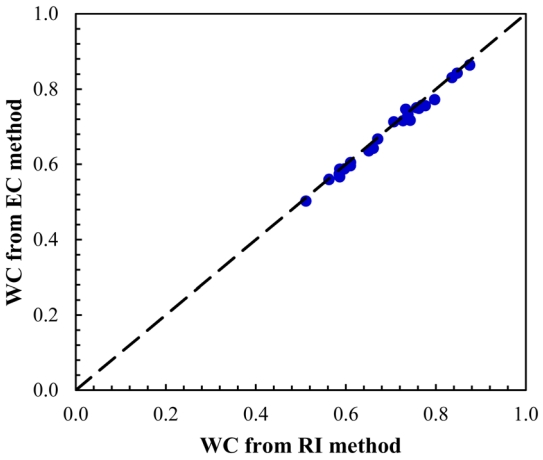

Fig. 10 Water cut obtained from EC *versus* water cut obtained from RI for unknown emulsion samples.

$$WC_i = \frac{V_{water,i}}{V_{emulsion,i}} \quad (14)$$

where $V_{water,i}$ and $V_{emulsion,i}$ are the volumes of water and emulsion for sample i, respectively.

The volumetric water cut (v/v) derived from the RI and EC measurements were very close to each other, as shown in SI Table A-9 and Fig. 10, and acceptably close to the corresponding values obtained using the centrifuge technique, as shown in SI Table A-9 and Fig. 11. A closer look at Fig. 10 reveals that the water cut measured by the EC method was generally 0.01 to 0.02 lower than that measured by the RI method. This difference is attributed to the fact that EC is a dynamic measurement influenced by ion mobility, which is hindered by the natural surfactant layer and trace organics remaining at the water–oil interface. These natural surfactants form a concentrated layer on the droplet surfaces that creates an "additional barrier for interphase ion transport", effectively complicating charge transfer across the emulsion.[30] Consequently, the EC method tends to underestimate salinity. In contrast, the RI method responds to total solute content, which is less sensitive to ionic mobility, allowing for more robust measurements in such conditions—especially when calibration

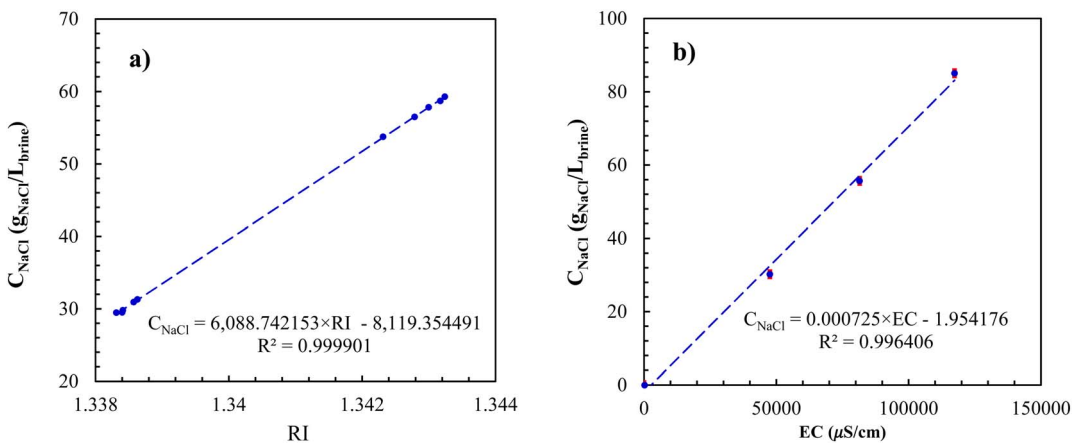

Fig. 9 (a) Salinity–RI calibration curve, (b) salinity–EC calibration curve for unknown emulsion samples.

© 2026 The Author(s). Published by the Royal Society of Chemistry

Open Access Article. Published on 27 May 2026. Downloaded on 5/30/2026 4:58:45 PM.
This article is licensed under a Creative Commons Attribution-NonCommercial 3.0 Unported Licence.

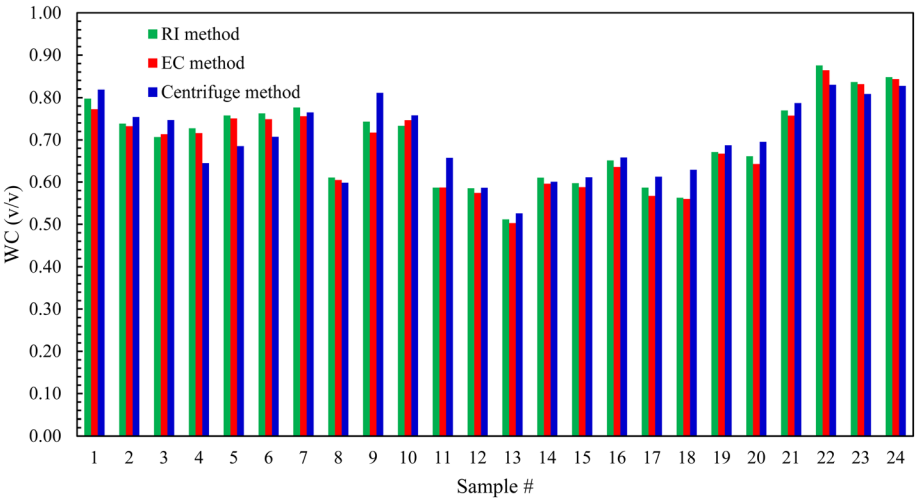

Fig. 11 Volumetric water cuts (v/v) obtained from the RI (green bars), EC (red bars), and centrifuge (blue bars) methods for the unknown emulsion samples.

includes realistic emulsion compositions. As shown previously, it is important to highlight that separating water from the oleic phase using the centrifuge technique is prone to significant human error, particularly in ensuring the complete removal of the separated aqueous phase. Additionally, there are inherent challenges in achieving full coalescence of dispersed micro- or nano-sized water droplets within the oleic phase or oleic droplets within the aqueous phase.

These limitations make the RI and EC techniques more accurate than the centrifuge method. As shown in SI Table A-9, the values obtained from these two methods are very close and do not require physical separation of water from the oleic phase. These results highlight the effectiveness of the RI and EC techniques relative to centrifuge-based volumetric calculations for water-cut measurements in stable emulsions.

6. Conclusion

This study introduces a novel methodology for measuring water cut in stable emulsions without the need for phase separation. By integrating Boyle's law with RI or EC techniques, this approach successfully avoids the errors typically caused by emulsion inhomogeneity and the difficulties of traditional physical separation.

Our findings confirm that Boyle's law provides a highly reliable measurement of total emulsion volume, outperforming standard volumetric methods. When characterizing the aqueous phase, the RI method proved to be the most robust, achieving accuracy within 2% and excellent repeatability, while eliminating the need for time-consuming water evaporation or vacuum-drying steps. While the RI method proved superior in precision, the EC method offers a strong complementary alternative, particularly for rapid screening in stable systems.

The robustness of this methodology was further validated using unknown samples from SAGD experiments, where results closely matched conventional centrifuge benchmarks. Overall, these techniques offer a significant leap in efficiency for fluid analysis in thermal recovery operations. Future research will focus on automating data acquisition and expanding the application of this separation-free framework to other complex industrial emulsions.

Conflicts of interest

There are no conflicts to declare.

Data availability

The data supporting the findings of this study are available within the article and its supplementary information (SI). Supplementary information: tables containing both raw and calculated data corresponding to the figures included in the main text. The supporting tables provide data for calibration samples and for known and unknown emulsion samples. Additional details about the prepared emulsions are provided beneath each corresponding table. See DOI: https://doi.org/10.1039/d6ra03130g.

Acknowledgements

The authors acknowledge the financial support of the Natural Sciences and Engineering Research Council of Canada (NSERC) and all the member companies of the SHARP Research Consortium: Canadian Natural Resources Ltd., Cenovus Energy, Imperial Oil Limited, Kuwait Oil Company, Strathcona Resources Ltd, and Suncor Energy. The support of the Department of Chemical and Petroleum Engineering and the Schulich School of Engineering at the University of Calgary is also acknowledged.

References

1 Y. Yang, Y. Xu, C. Yuan, J. Wang, H. Wu and T. Zhang, *Measurement*, 2021, **174**, 109078.

Open Access Article. Published on 27 May 2026. Downloaded on 5/30/2026 4:58:45 PM. This article is licensed under a Creative Commons Attribution-NonCommercial 3.0 Unported Licence.

2 G. Guowang, H. Dasen, L. Hua, F. Wang and Y. Li, *J. Phys.: Conf. Ser.*, 2021, **1894**, 012093.
3 Q. Liu, B. Chu, J. Peng and S. Tang, *Sensors*, 2019, **19**, 2963.
4 Y. Gong, G. Gao, P. Zhao, D. Wu, F. Wang and S. Yan, *4th International Conference on Intelligent Control, Measurement and Signal Processing (ICMSP)*, 2022, pp. 152–155.
5 E. Scholz, *Karl Fischer Titration: Determination of Water*, Springer Science & Business Media, 2012.
6 B. Kamal, Z. Abbasi and H. Hassanzadeh, *Energies*, 2023, **16**, 6410.
7 S. Yurish, *Advances in Measurements and Instrumentation: Reviews*, International Frequency Sensor Association Publishing, 2018, vol. 1.
8 S. Castrup, *SPE Western Regional Meeting*, 2021, DOI: 10.2118/200797-MS.
9 N. Reinecke, G. Petritsch, D. Schmitz and D. Mewes, *Chem. Eng. Technol.*, 1998, **21**, 7–18.
10 I. Ismail, J. Gamio, S. A. Bukhari and W. Yang, *Flow Meas. Instrum.*, 2005, **16**, 145–155.
11 R. Thorn, G. A. Johansen and B. T. Hjertaker, *Meas. Sci. Technol.*, 2012, **24**, 012003.
12 C. Sætre, G. Johansen and S. Tjugum, *Flow Meas. Instrum.*, 2010, **21**, 454–461.
13 W. Kumara, B. Halvorsen and M. Melaaen, *Int. J. Multiphase Flow*, 2010, **36**, 467–480.
14 L. S. Hansen, S. Pedersen and P. Durdevic, *Sensors*, 2019, **19**, 2184.
15 T. Nassereddin, K. Al Hagin, M. Hariz, M. Melo, B. Raman and R. Helal, *Abu Dhabi International Petroleum Exhibition and Conference*, 2021.
16 B. Khamis and B. Haridas, *SPE Annual Technical Conference and Exhibition*, 2003.
17 T. O'Banion, *Chem. Eng. Prog.*, 2013, **109**, 41–46.
18 M. Al-Amri, F. Al-Khelaiwi and M. Al-Kadem, *Abu Dhabi International Petroleum Exhibition and Conference*, 2012.
19 C. Teixeira, L. Da Silva, G. Veloso, G. Lambert-Torres, M. Campos, I. Noronha, E. Bonaldi and L. De Oliveira, *Measurement*, 2019, **148**, 106907.
20 A. Chaudhuri, D. Sinha, A. Zalte, E. Pereyra, C. Webb and M. Gonzalez, *J. Fluid Eng.*, 2014, **136**, 031304.
21 A. Hamouda, O. Manck, M. Hafiane and N. Bouguechal, *Sensors*, 2016, **16**, 1008.
22 B. Kamal, S. Vestrum, M. BinDahbag, Z. Abbasi and H. Hassanzadeh, *Measurement*, 2024, **228**, 114314.
23 C. Yuan, A. Bowler, J. Davies, B. Hewakandamby and G. Dimitrakis, *Sens. Actuators, B*, 2019, **298**, 126886.
24 M. Al-Kizwini, S. Wylie, D. Al-Khafaji and A. Al-Shamma'a, *Measurement*, 2013, **46**, 45–51.
25 X. Liu, J. Hu, F. Shan, B. Cai, X. Su and Q. Chen, *Chem. Eng. Commun.*, 2009, **197**, 232–238.
26 Reichert Analytical Instrument. Abbe MARK III Refractometer user guide manual (Reprint), 2010, https://www.manualslib.com/manual/2134224/Reichert-Abbe-Mark-Iii.html#manual.
27 Cond probe In Lab 731-ISM, https://www.mt.com/ph/en/home/products/Laboratory_Analytics_Browse/pH-meter/sensor/conductivity-sensor/InLab-731-ISM.html, (accessed November 12, 2024.
28 Ohaus Adventurer Pro AV264C Manual. US (Reprint). https://www.mse.ucr.edu/media/491/download.
29 VWR 1400E Scientific Economy Vacuum Oven. US (Reprint). https://www.artisantg.com/53421-1.
30 A. Zakinyan, L. Kulgina, A. Zakinyan and S. Turkin, *Fluid*, 2020, **5**, 74.

© 2026 The Author(s). Published by the Royal Society of Chemistry